Proceedings of IDETC/CIE 2005
ASME 2005 International Design Engineering Technical Conferences
& Computers and Information in Engineering Conference
September 24-28, 2005, Long Beach, California USA

DETC2005-85241

DYNAMIC MODELING AND CONTROLLER DESIGN OF A PLANAR PARALLEL 3-RRR COMPLIANT MICROMANIPULATOR

Jingjun Yu[1], Dong Zhao[2] Shusheng Bi[1], and Guanghua Zong[1]
[1]**Robotics Institute, Beijing University of Aeronautics and Astronautics, Beijing, 100083, China**
[2]**Department of Mechanical and Aerospace Engineering, University of Florida, USA**

ABSTRACT

This paper presents control system formulations of a planar parallel 3-RRR parallel compliant micromanipulator. The design methodology is illustrated with one of such designs constructed at Beijing University of Aeronautics and Astronautics, China. Compliant joints and motion-amplifying mechanism allow rapid and accurate response as well as larger workspace. The three PZT actuators attached on the linkages produce the bending moments. The sensor is a CCD camera feeding back the tool point position. The plant is the equations of motion which can be formulated using the Lagrangian method and dynamics software. The system dynamic model was developed with ADAMS which can export the nonlinear and linearized control plant to Matlab Simulink. Overall dynamic behavior of the manipulator will be illustrated through simulations with Matlab Simulink Toolbox. After comparison of two different control plans, the controller obtained from LQR method was chosen to achieve the control objectives. Closed-loop performance in response to a step reference was plotted. Bode plots of the sensitivity and complementary sensitivity showed their relation to the step response. Gain and phase margins was computed.

KEYWORDS: Compliant Mechanism, Flexure Hinge, Dynamics, Controller, Parallel Mechanism

INTRODUCTION

Parallel mechanism (PM) has the following advantages over serial one: more rapid response, higher accuracy, better stiffness and lighter weight. A principle drawback of the PM is the reduced workspace. Compliant joint (CJ), also frequently called flexure hinge[1], achieves the same motion as regular joint by the elastic deformation of the material. Mechanism with CJs has very high positioning accuracy because of no backlash at the joints. Taking the advantages of both PM and CJ, a parallel compliant micromanipulator (PCMM) can be designed to obtain high positioning accuracy (typically 0.1 μ m). This micromanipulator can be applied to microassembly in semiconductor industry and micromanipulation in bioengineering, like cell operation, which require high accuracy with small workspace.

Currently, only few successful applications of multi-DOF PCMMs have been demonstrated in the literature. Examples include Pernette[2], Arai[3], Goldfarb[4], Canfield[5], and Zhang[6] et al. They analyzed parallel compliant micromanipulators with pseudo-rigid-body model(PRBM) methods[7] which assume CJs behave as revolute joints with torsional springs attached while the thicker section of the mechanism behave as rigid links. As a basic tool necessary to model, design, and control the compliant micromanipulator, the pseudo-rigid-body model allows compliant mechanisms to be analyzed using well-known rigid-body kinematics.

A planar PCMM, whose rigid-body counterpart is a well-known planar three-DOF[X, Y, θ] 3-RRR PM, has many advantages such as compact structure and simple kinematics. In addition, all kinematic pairs can be designed as compliant revolute joints to avoid backlash and hysteresis. Moreover, it can be manufactured into a monolithic structure. Numerous literatures discuss the kinematics of the 3-RRR PCMM based on its PRBM[8-10], but dynamic models and the corresponding controller design of PCMM were studied less frequently. Wang et al.[11] outlined a method to derive the kinematics and dynamics of a 6-DOF micromanipulator that used a 3-RRR stage. Their method used vector analysis and the Lagrangian method, resulting in a non-linear dynamic model. Zhang et al.[6] developed a constant Jacobian method for modelling the kinematics of a 3-RRR PCMM, which proved to be as accurate as a non-linear kinematic model. Further to this work Zou[12]

applied the Lagrangian method to derive a dynamic model of the same compliant 3-RRR mechanism and Handley[13] presents a simple method to derive a linear dynamic model for 3-RRR PCMM which may be used in structure/controller optimization. Ryu et al.[14] also discussed the dynamic modeling of a 3-RRR PCMM to be used for optimal design. They suggested application of the Lagrangian method but did not discuss the derivation of the stiffness and inertia. As yet there is no discussion in the literature of general methods to design controller for the PCMM based on the derived dynamic model.

A 3-RRR PCMM with motion-amplifying mechanism was constructed at Beijing University of Aeronautics and Astronautics, China. This paper studies design and control of this mechanism with the aid of ADAMS (MSC. Software) and Matlab Simulink (Mathworks, Inc.). Forward kinematic derivation was done to decide the critical joint locations that should be optimized. Optimization of PCMM dynamic model developed with ADAMS was performed. Both linear and nonlinear plants of the system were exported to Simulink. For such a high accurate device, the disturbance from the environment can not be neglected. Two PID controllers were constructed to minimize the overshoot and settling time for response to a step response and improving the disturbance rejection. Pole placement method was adopted to find the control elements of the linearized control plant. Then the controllers were applied to the nonlinear plant. The method presented in this paper can be also applied for kinematic analysis and controller design for the other PCMMs.

KINEMATICS OF THE 3-RRR PCMM

The CAD model and kinematic diagram of the planar 3-RRR PCMM with motion-amplifying mechanism are shown in Fig. 1 and Fig. 2. The three passive revolute joints are located on the moving platform at C_i, where i = 1, 2, 3. The active revolute joints are located at the E_i. The motion-amplifying mechanism consists of link D_iE_i and link A_iB_i. OT is a bar fixed to the moving platform for visualization of the motion. This mechanism has 3 degree-of-freedom (DOF). Although there are a link and translational joint at D_i, the real design did not implement that link and translational join. The translational motion can be achieved by the deformation of the CJ at D_i.

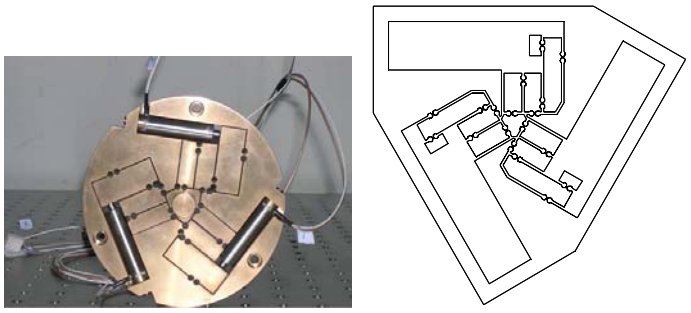

(a) (b)

Fig. 1 (a) Photo of a planar 3-RRR PCCM with PZT actuators; (b) CAD model of Kinematic diagram of the PCCM with motion-amplifying mechanism.

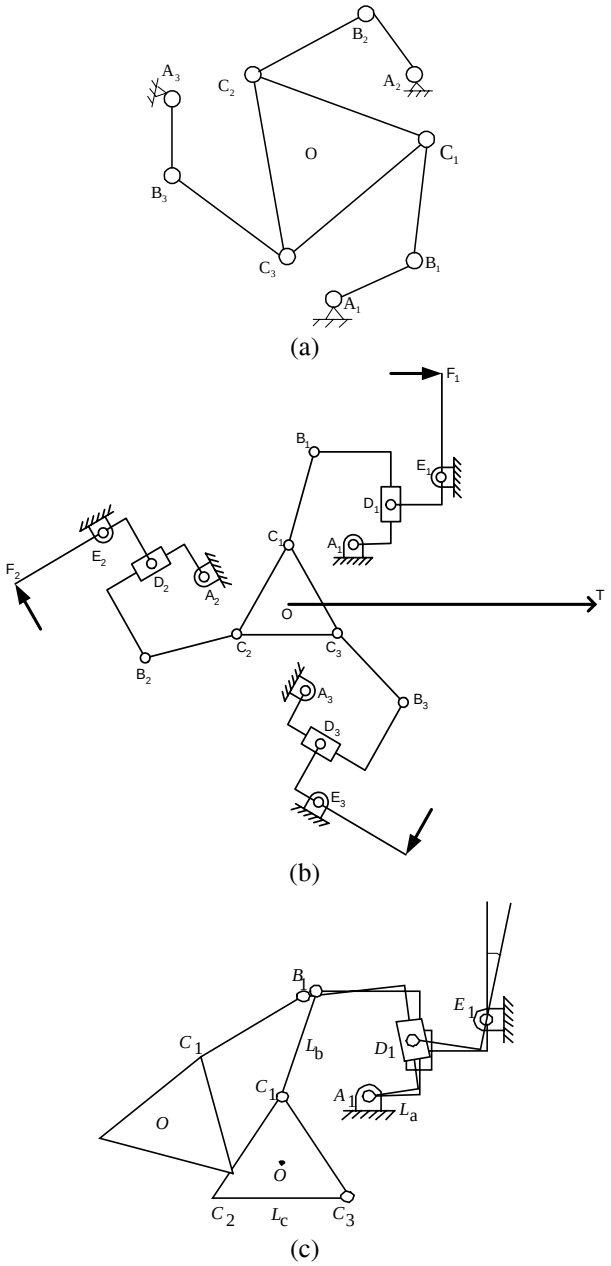

Fig. 2 (a) Equivalent rigid-body kinematic diagram of Planar 3-RRR PCMM; (b) Kinematic diagram of Planar 3-RRR PCMM with motion-amplifying mechanism (linkage D_iE_i, i =1,2,3), (c) Kinematic diagram of one leg

It is easy to derive the position of O' and orientation of the platform given the 3 input angles θ_i (Fig. 3). The coordinates of point B_i can be obtained from the geometry relationship.

$$\begin{Bmatrix} x_{B_i} \\ y_{B_i} \end{Bmatrix} = g(A_iB_i, D_iE_i, \theta_i) \tag{1}$$

With the three calculated coordinates of the B_i, the position of O' can be calculated.

$$\begin{Bmatrix} x_{O'} \\ y_{O'} \end{Bmatrix} = f(l_3, a, x_{B_i}, y_{B_i}) \qquad i = 1,2,3 \tag{2}$$

which the new position of the center of the platform and the C_i, the orientation can also be computed.

KINEMATIC OPTIMIZATION

The combination of all the link length and locations of the revolute joint decides the position and orientation of the tool point. These could be the design variables of the optimization of the workspace. Depending on the application of this PM, the objective function could be to maximize the displacement of O or the rotation angle of the platform.

With three identical applied motions at joints E_i being inputs and the angle limits of the joints being constraints, the optimizations were performed with ADAMS as shown in Fig. 3.

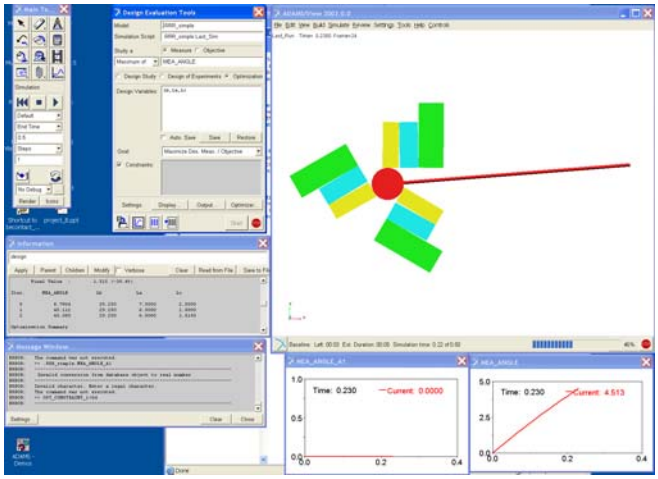

Fig. 3 ADAMS optimization snapshot

If the objective function is to maximize the rotation of the platform with three identical inputs at joints E_i, the results are shown in Table 1. L_a, L_b and L_c are the location of the joints in their local frames.

Table 1. Optimization results of maximum of rotation angle.

Design Variables	L_a(mm)	L_b(mm)	L_c(mm)
Initial Value	7.5	28.25	2.5
Final Value	6.5 (-13.3%)	29.25(+3.54%)	1.515(-39.4%)

If the objective function is to maximize the displacement of the tool point in X direction with an input at joints E_1, the results are show in Table. 2.

Table 2. Optimization results of maximum of displacement.

Design Variables	L_a(mm)	L_b(mm)	L_c(mm)
Initial Value	7.5	28.25	2.5
Final Value	7.5(+0%)	28.25(+0%)	2.515(+0.6%)

DYNAMIC MODEL

Assume the links of the planar 3-RRR PCMM being rigid and compliance is only in the joints. Ignore the actuator force coupling on the three actuators. The equation of motion can be obtained with Lagrangian method.

$$\frac{d}{dt}\left(\frac{\partial L}{\partial \dot{q}_i}\right) - \frac{\partial L}{\partial q_i} = Q_i \qquad i = 1, 2, \cdots n \tag{3}$$

where

$L = K - P$, K is the kinetic energy; P is the potential energy.

Q_i is the generalized force.

q_i is the generalized coordinate.

n is the number of degree of freedom of the manipulator.

For this planar 3-RRR PCMM, the generalized coordinates can be chosen as the three displacements $(\Delta l_1, \Delta l_2, \Delta l_3)$ of the PZT actuators. The potential energy is from elastic deformation of all the CJs. The generalized forces are the three actuate forces generated by the PZT with the no force coupling assumption.

With some algebra, the equation of motion of this system can be obtained in the form of Eq.(4). It can also be calculated automatically with an ADAMS model of this system.

$$M(q)\ddot{q} + H(q, \dot{q}) + G(q) = Q \tag{4}$$

A dynamic model of the PCMM was developed in ADAMS with the dimensions from the real part. The mass and inertial of each link can be calculated automatic from the geometry of the mechanism. Since it is hard to make complex geometry in ADAMS, geometry model of each link can be developed with Pro/Engineer (Fig. 4) to get the mass and inertial properties. It will be convenient to refine the design with parametric modeling software like Pro/Engineer.

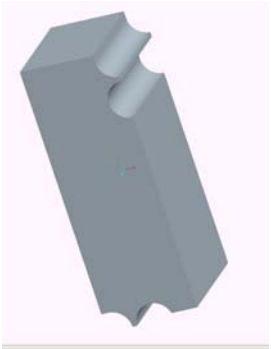

Fig. 4 Pro/Engineer model of link BC for getting the mass and inertial

In the ADAMS model (Fig. 5 and Fig. 6), the CJ was modeled as a pin joint with torsion spring. The values of stiffness and damping of the torsion spring can be obtained experimentally or theoretically. Actuator force was modeled as body moving applied force. By fixing one of translational motions of the planar joint, the joint at point D can be modeled. Note that the translational motion must be very small to

simulate the real CJ. Rotational joint motions were applied on the joint E_i for kinematic study. The actuator force and applied motion can be switched by deactive/active them.

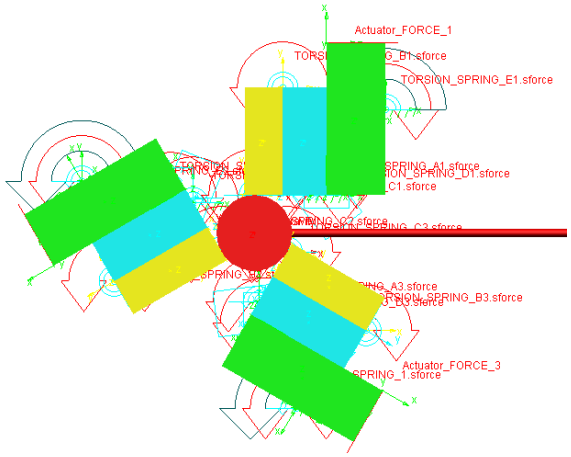

Fig. 5 Dynamic model of the PCMM system

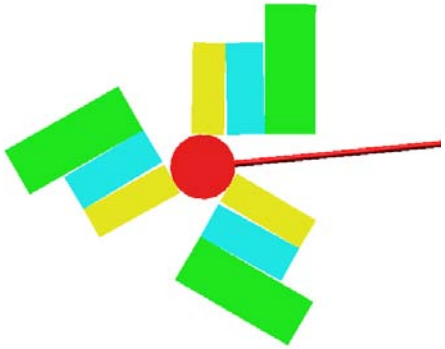

Fig. 6 Dynamic simulation results

CONTROLLER DESIGN

Actuator and sensor

Three piezoelectric actuators (PZT) enable this PCMM high position accuracy at the magnitude of μm. The three piezoelectric actuators apply their linear force at points F_i resulting the bending moment at joints E_i. Since the mechanism is so small, there is no space for regular position or force sensors. CCD camera will be used as sensor to get the position. If the sampling frequency of the image processing system is high enough, the velocity and acceleration information can be calculated by with time derivative at each time frame. A bar *OT* is fixed to the center of the moving platform which presenting the end-effector (Fig. 2).

Design objectives

Two plans i.e. Pole placement (Fig. 7) and LQR method (Fig. 8) were employed in order to achieve the following objectives for response to step reference.

- Overshoot is less than 20%.
- Settling time is less than 1 second.
- No steady-state error.
- Response to an impulse disturbance decays quickly to zero.
- Guarantee classical robustness of the system (Gain margin at least 6 dB, phase margin at least 45 degree).

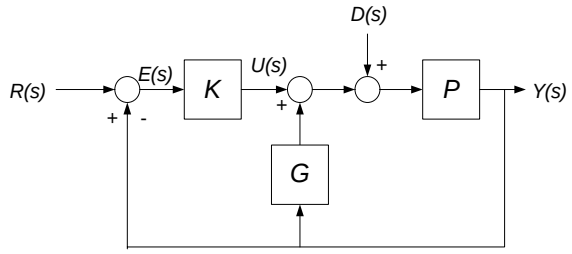

Fig. 7 Control block diagram of Plan A: Pole placemen

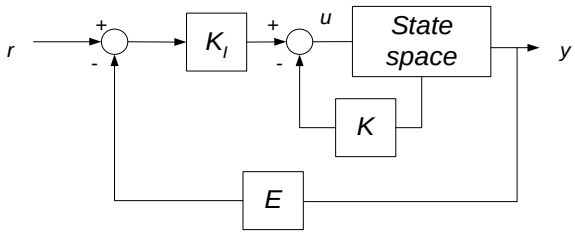

Fig. 8 Control block diagram of Plan B: LQR method

Transfer function (TF) of Plan A

Define only one input of system when exporting the model from ADAMS to Simulink. The transfer functions of each loop of the Plan A (Fig. 7) are as follows.

$$TF1 = \frac{Y(s)}{R(s)} = \frac{P(s)K(s)}{1 + P(s)[K(s) + G(s)]} \quad (5)$$

$$TF2 = \frac{Y(s)}{D(s)} = \frac{P(s)}{1 + P(s)[K(s) + G(s)]} \quad (6)$$

where $P(s)$ is the linearized control plant. ADAMS can automatically output the linearized state space plant. The frequency domain plant can be derived from it. $K(s)$, $G(s)$ are the unknown control elements.

To achieve the design objectives for response to step reference, the characteristic equation of a second order system can be used. The controller can be designed with dominant second order poles.

The desired characteristic equation is

$$s^2 + 2\zeta\omega_n s + \omega_n^2 \quad (7)$$

which fulfils

(a). Overshoot:

$$M_p = e^{-\frac{\pi\zeta}{\sqrt{1-\zeta^2}}} < 0.2 \quad (8)$$

where $0<\zeta<1$

(b). Settling time:

$$t_s = \frac{3}{\zeta\omega_n} < 0.1 \quad (9)$$

So the range of the damping ratio and natural frequency can be computed.

$$0.456 < \zeta < 1 \quad (10)$$

$$\omega_n > 65.80 \quad (11)$$

Controller design of Plan A

$K(s)$ and $G(s)$ are designed as PID controllers.

$$K(s) = K_{P1} + \frac{K_{I1}}{s} + K_{D1}s \quad (12)$$

$$G(s) = K_{P2} + \frac{K_{I2}}{s} + K_{D2}s \quad (13)$$

Substituting $K(s)$ and $G(s)$ into Eq. (5) and Eq. (6), the denominator of the transfer function for the input reference is

$$D(s) = s^7 + c_6 s^6 + c_5 s^5 + c_4 s^4 + c_3 s^3 + c_2 s^2 + c_1 s^1 + c_1 \quad (14)$$

The coefficients of the denominator are function of the unknown control elements. So the transfer functions have 7 poles. The conjugate poles (p_1 , p_2) of the second order system can be obtained from $\alpha = \xi\omega_n$ and $\omega = \omega_n\sqrt{1-\zeta^2}$. Then, by selecting the other insignificant poles ($P_i, i = 3,4,...7$), a new characteristic equation can be derived.

$$(s-p_1)(s-p_2)\ldots(s-p_7) = s^7 + c_6 s^6 + c_5 s^5 + c_4 s^4 + c_3 s^3 + c_2 s^2 + c_1 s^1 + c_1 \quad (15)$$

Then by matching the coefficients of the characteristic equation, the control elements can be obtained. The dominant poles shown in Fig. 9 can be selected in the stable region.

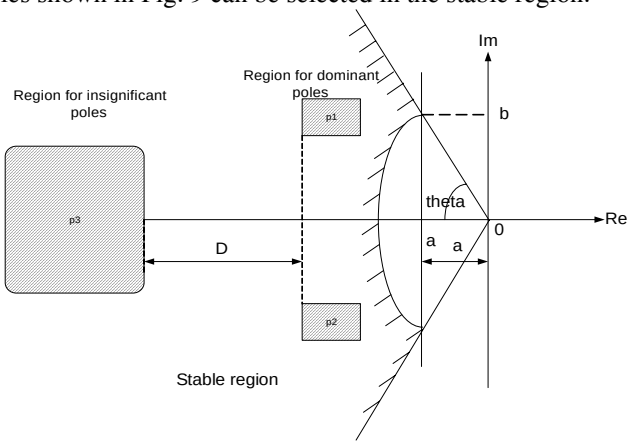

Fig. 9 Regions of dominant and insignificant poles in the s-plane (The *D* is the distance between the dominant region and the least-significant region. The magnitude of the insignificant pole is at least 5 to 10 times that of a dominant pole.)

For this model,

$$\zeta\omega_n > 30 \quad (16)$$

From

$$\theta = a\cos(\xi) \quad (17)$$

The range of θ is

$$0 < \theta < 62.87° \quad (18)$$

By choosing the closed-loop poles in the stable region (Fig. 9), the coefficients c_i of the characteristic equation can be calculated and the controller elements can be obtained. This plan only works for the single input. For such a high order system, it is very hard to do the calculation, so the Ackermann's method was employed to find the constant gain matrix controller. After all the gains were obtained, combining them to implement the control system shown in Fig. 10.

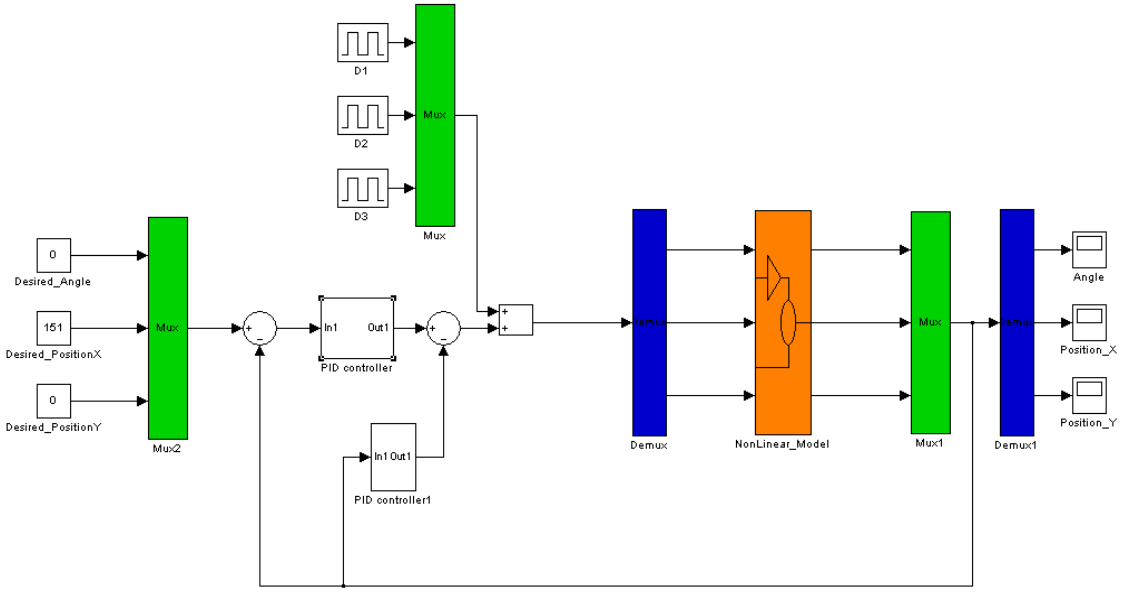

Fig. 10 Implementation of the control system shown in Fig. 8 with Simulink.

Controller design of Plan B

All the states are needed to design the controller with LQR method. So the state space transfer function was constructed as Fig. 11 given the matrices *A*, *B*, *C*, and *D*. All the states can be feedbacks.

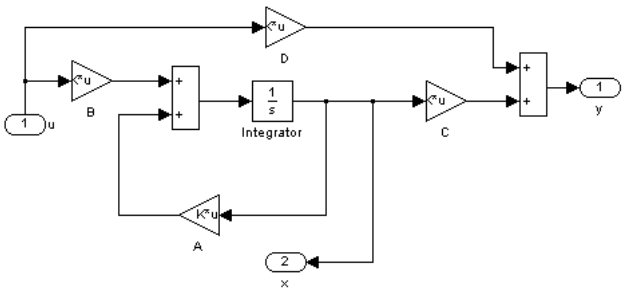

Fig. 11 Implementation of the state space transfer function subsystem for feeding back all states.

There is no integrator $\frac{1}{s}$ term in the transfer function of the plant. So a feed forward integrator is needed. For this MIMO system, new *A*, *B*, *C*, and *D* need to be derived to use the LQR method to find the gains. Define the $\dot{a}$ and a as in Fig. 12.

$$\begin{cases} \dot{x} = Ax + Bu \\ y = Cx + Du \end{cases} \tag{19}$$

So

$$\begin{cases} u = -Kx + K_I \dot{a} \\ \dot{a} = r - y = r - ECx - EDu \end{cases} \tag{20}$$

If it is a steady-state system and input is a step function, it can be derived as follows.

$$\dot{e} = A_{new} e + B_{new} ue \tag{21}$$

So the new A, B, C and D can be obtained.

$$A_{new} = \begin{bmatrix} A & 0 \\ -EC & 0 \end{bmatrix} \qquad B_{new} = \begin{bmatrix} B \\ -ED \end{bmatrix} \tag{22}$$

Apply the LQR function, the gains can be calculated.

$$K_{new} = [K \vdots -K_I] \tag{23}$$

The discrete time model is shown in Fig. 13.

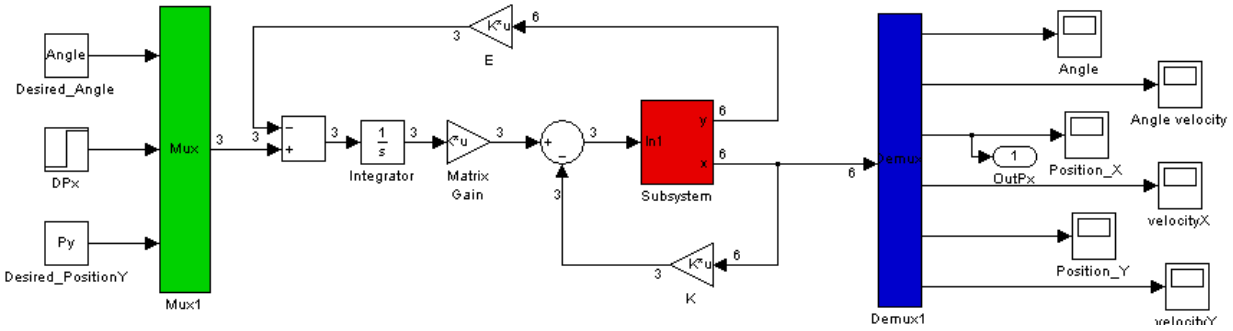

Fig. 12 Implementation of the controller with the LQR method.

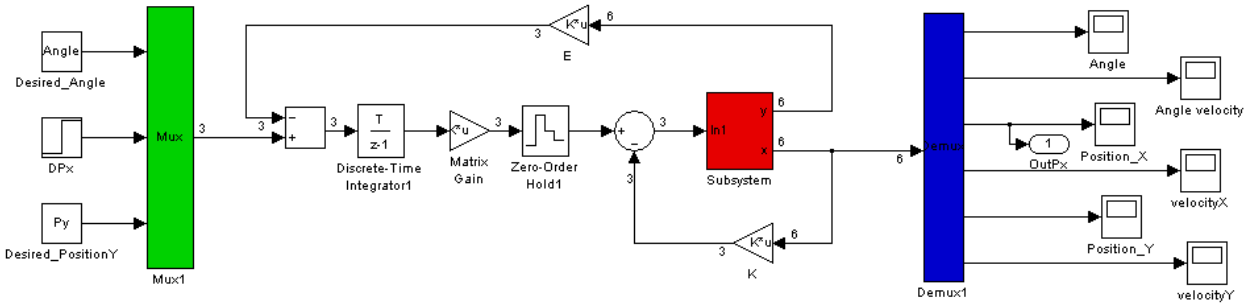

Fig. 13 Implementation of the discrete time controller with the LQR method.

RESULTS

Choose the *X* position of the tool point as the most concerned output because it is the most wanted motion in applications like cell injection. One of the PID controller parameters are shown is Table 3. However, the system response with these setting did not satisfy the design objective.

Table 3. Gains of the *K* PID controller of the system

	Input1	Input2	Input3
K_P	29862.06	71530.50	31287.90
K_D	18987.88	64668.82	39957.07

LQR method can give much better system response as shown in Fig. 14. Set the *X* poison input as a step of 0.45 and set the input angle and position Y as zero. The control elements are as follows.

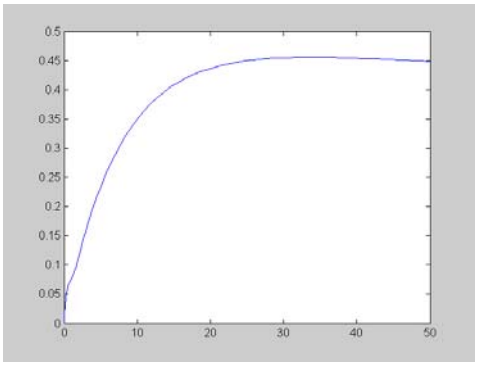

Fig. 14 Step response to a 0.45 step reference with the model from LQR method.

Sensitivity and complementary sensitivity derivation for the PID control system

Sensitivity

$$S = \frac{dTF1}{dP}\frac{P}{TF1} = \frac{1}{1+PK} \tag{24}$$

Complementary sensitivity

$$T = 1 - S = \frac{PK}{1+PK} \tag{25}$$

Make the bode diagram with Matlab as shown in Fig. 16.

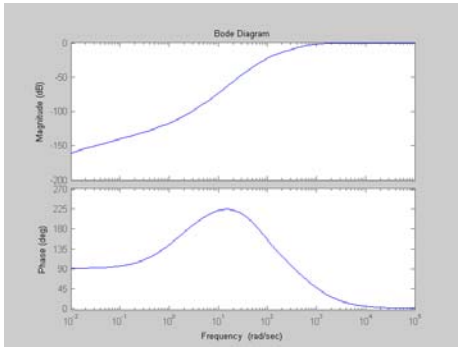

(a)

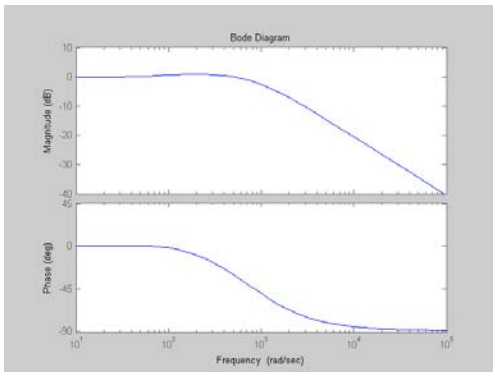

(b)

Fig. 15 (a) Bode plot of Sensitivity; (b) Bode plot of complementary sensitivity.

Gain and phase margins for the PID controller

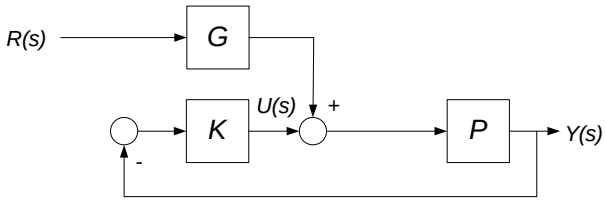

(a)

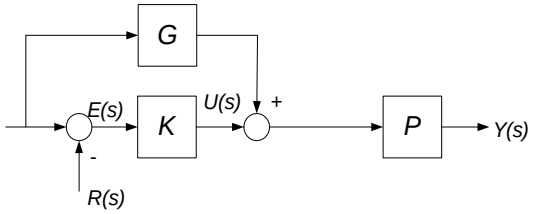

(b)

Fig. 16 Open loop block diagram for the first loop; (a) and second loop (b).

For the first loop of the first model, the open loop model is

$$SYS1 = \frac{G(s)P(s)}{1 - K(s)P(s)} \tag{26}$$

For the second loop

$$SYS2 = -K(s)P(s) \tag{27}$$

The Bode Diagrams of this open loop systems are shown in Fig. 17. The gain margins and phase margins are shown in Table 4.

Table 4. Gain margins and phase margins

	Gain margin	Phase margin (deg)
Loop1 (*SYS1*)	3107.1	Inf
Loop2 (*SYS2*)	Inf	-98.0

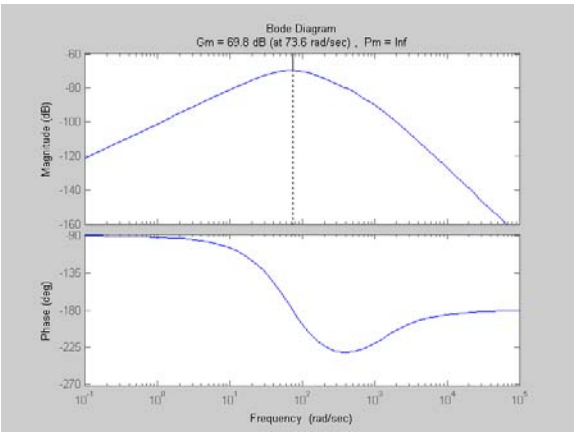

(a)

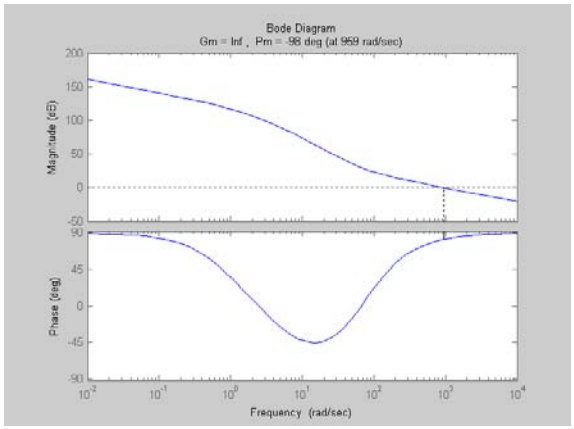

(b)

Fig. 17 Bode plots for the gain margin and phase margin (a) *SYS*1 and (b) *SYS*2.

CONCLUSIONS

This paper presents the methodology of dynamic modeling and controller design of the planar 3-RRR PCMM. The design was evaluated with ADAMS. ADAMS is a dynamics software for kinematic design optimization and controller design.

To model a CJ, the value of stiffness and damping of the torsion spring is critical. The values can be obtained experimentally or theoretically. It will be a great contribution if there is formula derived given the material property and geometry of a CJ. If there is a desired work envelop for specific application, it might be achieved with asymmetric design. The controller design for such a nonlinear high order system is hard to do. Linear quadratic regulator (LQR) could be a good choice for the controller of this plant.

ACKNOWLEDGMENTS

The authors would like to acknowledge the support of National Science Foundation of China, through Grant No. 50405007 and 50475002.

REFERENCES

1. J. M. Paros and L. Weisbord, “How to design flexure hinges, Machine Design”, 1965, 37, 151-156
2. E. Pernette, S. Henein, I. Magnani, et al., “Design of Parallel Robots in Microrobots”, Robotica, 1997, Vol.15, 417-420
3. Tanikawa T, Arai T, and Koyachi N. “Development of Small-size 3 DOF Finger Module in Micro Hand for Micro Manipulation”, Proceedings of the IROS, 1999, 876-881
4. J.E. Speich, M. Goldfarb, “Compliant manipulator design for spatial micromanipulator”, Proceeding of IARP 2nd International Workshop on Micro Robotics and Systems, Beijing, China, 1998, 93-103
5. S.L. Canfield, J.W. Beard, N. Lobontiu, et.al. “Development of a spatial compliant manipulator”, International Journal of Robotics and Automation, 2002, Vol. 17, No. 1: 63-71
6. W. J. Zhang, J. Zou, G. Watson, W. Zhao, G. Zong and S. Bi, “Constant-Jacobian Method for Kinematics of a 3-DOF Planar Micro-Motion Stage”, Journal of Robotic Systems, 2002, 19(2): 63-79
7. Howell, L. L., and Midha, A., “A Method for Design of Compliant Mechanisms with Small-Length Flexible Pivots”, Transactions of the ASME, Vol.116, 1994, 280-289
8. B. J. Yi, G. B. Chung, H. Y. Na, et al. “Design and Experiment of a 3-DOF Parallel Micromechanism Utilizing Flexure Hinges”, IEEE Transactions on Robotics and Automation, 2003, Vol. 19, No. 4, 604-612
9. J. Hesselbach and A. Raatz, “Pseudoelastic flexure-hinges in robots for micro assembly”, Proc. SPIE Microrobotics and Microassembly II, Vol. 4914, 2000, pp. 157-167.
10. J. J. Yu, S. S. Bi, and G. H. Zong, “A method to evaluate and calculate the mobility of a general compliant parallel manipulator”, ASME 2004 DETC, Salt Lake City, USA, 2004, MECH-57283
11. S. Wang, G. Zong, S. Bi and W. Zhao, “Dynamics analysis of a 6-dof serial-parallel micromanipulator”, IEEE 1997 International Symposium on Micromechatronics and Human Science, 1997, 191-197
12. J. Zou, “Kinematics, Dynamics and Control of a Particular Micro-Motion System”, Masters Thesis, printed by the Advanced Engineering Design Laboratory, University of Saskatchewan, 2000
13. D. C. Handleya, T. F. Lu, Y. K.. Yonga, W. J. Zhang, “A simple and efficient dynamic modelling method for compliant micropositioning mechanisms using flexure hinges” Proceedings of SPIE, Vol.5276, Device and Process Technologies for MEMS, Microelectronics, and Photonics III, 2004, 67-76
14. J. Ryu, D. Gweon and K. Moon, “Optimal design of a flexure hinge based XYθ wafer stage”, Precision Engineering, 1997, 21: 18-28